

# Correlated vibrational frequencies of polymers: MBPT(2) for all-*trans* polymethineimine

Jun-Qiang Sun and Rodney J. Bartlett

*Quantum Theory Project, Departments of Chemistry and Physics, University of Florida, Gainesville, Florida 32611*

(Received 11 April 1997; accepted 26 September 1997)

Polymethineimine is a conjugated polymer, isovalent with polyacetylene, which was first synthesized in 1971. It has been found to be a semiconductor, though prior theory did not support that. Except for its vibrational frequencies which have been measured, little about the polymer is known. MBPT(2) is applied to calculate its equilibrium structure, band gap, and vibrational frequencies. The latter represents the first time an *ab initio* correlated method has been applied to this problem for an infinite system. The calculations for three basis sets, STO-3G, 6-31G, and 6-31G\*\* demonstrate that both basis and electron correlation have a strong influence on its optimized geometry. The MBPT(2) band gap with a polarized basis set (6-31G\*\*) is 4.7826 eV, compared to 8.54 for Hartree-Fock. According to our MBPT(2) calculations, the band gap of all-*trans* polymethineimine would be estimated to be about 1 eV larger than that of polyacetylene, i.e.  $\sim 2.75 \pm 0.5$  eV. Electron correlation is demonstrated to have an important effect on the computed vibrational frequencies, which we find to be in good agreement with experiment.  
© 1998 American Institute of Physics. [S0021-9606(98)01601-8]

## I. INTRODUCTION

Polymethineimine was first synthesized in the early seventies by Wöhrle.<sup>1</sup> It is the prototype of a class of polymers which possess conjugated carbon-nitrogen double bonds. Conductivity measurements indicate that polymethineimine is a semiconductor,<sup>2</sup> making it a potential organic conductor with doping.<sup>3</sup> It also has interesting non-linear optical properties because it has an asymmetric monomer.<sup>4</sup> However, except for its three vibrational frequencies,<sup>1,2</sup> little about this polymer has been measured.

Karpfen<sup>5</sup> and Teramae *et al.*<sup>6</sup> have calculated the stable structure for polymethineimine using the Hartree-Fock (HF) method with basis sets 6-31G and STO-3G, respectively. Their results yielded a conjugated structure for the polymer, but there were obvious numerical differences among the two calculations since the basis sets used in their calculations were not large enough to obtain converged results, nor did their calculations include electron correlation which is likely to be critical in determining the equilibrium structures and other properties, especially for unsaturated systems.

For the band gap, empirical,<sup>7</sup> semi-empirical,<sup>8</sup> and HF (Ref. 6) methods have been applied to polymethineimine, with HF theory giving the largest band gap. From the HF calculation mentioned above, Teramae *et al.*<sup>6</sup> concluded that polymethineimine was unlikely to be an organic conductor with doping. However, this contradicts the observed semiconducting behavior of the system.<sup>2</sup>

Vibrational frequencies<sup>9</sup> of a system provide important information about the system's structure, as they are very sensitive to it. They become even more important when the equilibrium structure is not known. Vibrational frequencies are also important properties for either finite molecules<sup>9</sup> or infinite chains.<sup>10</sup> Since they are determined by the second derivatives of potential energy surfaces, they are sensitive to

the accuracy of the theoretical method and the size of basis set.<sup>11</sup> Few vibrational frequency calculations using *ab initio* methods have been done for infinite chains,<sup>6,12</sup> and all of those calculations were performed at the HF level or lower.<sup>6,12</sup>

Teramae *et al.*<sup>6</sup> obtained the frequencies for polymethineimine using HF in a STO-3G basis set, scaling with a factor of 0.89. However, lacking electron correlation and basis set flexibility in their calculation, little can be said about the convergence of the calculation.

Many-body perturbation theory (MBPT) (Ref. 13) and its infinite-order generalization, coupled cluster (CC) theory,<sup>14</sup> have proved to be effective and systematic ways to introduce electron correlation for molecules.<sup>11</sup> Second-order MBPT [MBPT(2)] has already been applied in extended systems to improve band gaps.<sup>15,16</sup> Most recently, MBPT(2) accurately explained the x-ray (XPS) and ultra-violet (UPS) photoelectron spectra of polyethylene and resolved long standing discrepancies among different experiments.<sup>17</sup> It is expected that MBPT(2) with a large basis set can provide reliable equilibrium structures, better predictions of the band gap, and a better understanding of the vibrational motion in polymethineimine.

In this report, we apply MBPT(2) to polymethineimine to determine its equilibrium structure, its band gap, and, particularly, its vibrational frequencies. Our objective is to assess the effect of the simplest level of correlation on the phonon spectra.

The plan of the paper is as follows. In Sec. II, we will briefly describe the procedure for geometry optimization in extended systems, then we will give the basic formulas for the band gap calculation, and finally we will discuss the calculation of vibrational frequencies in infinite, periodic systems. In Sec. III, we will apply the theory described in Sec. II

to polymethineimine to determine its equilibrium structure, its band gap, and vibrational frequencies. Then we will follow with conclusions.

## II. THEORY

### A. Geometry optimization

For a one-dimensional periodic system, the independent variables to describe the nuclear structure are the internal coordinates in one unit cell and the unit cell length  $a$ . If the symmetry of the system is larger than just the translational symmetry, the number of independent coordinates can be further reduced. Using  $\mathbf{r} = \{r_1, r_2, \dots, r_m\}$  to denote the independent internal coordinates of the polymer, then the Hartree-Fock (HF) total energy per unit cell  $E_{\text{uc}}^{\text{HF}}$  and the MBPT(2) total energy per unit cell  $E_{\text{uc}}^{\text{MBPT}(2)}$  for a given basis set are functions of  $r_1, r_2, \dots, r_m$ .

$E_{\text{uc}}^{\text{MBPT}(2)}$  is the sum of  $E_{\text{uc}}^{\text{HF}}$  and the second-order MBPT correction to the total energy per unit cell,  $E_{\text{uc}}^{(2)}$ , e.g.,

$$E_{\text{uc}}^{\text{MBPT}(2)} = E_{\text{uc}}^{\text{HF}} + E_{\text{uc}}^{(2)}. \quad (1)$$

The explicit expression for  $E_{\text{uc}}^{(2)}$  is<sup>16</sup>

$$E_{\text{uc}}^{(2)} = \frac{1}{W^3} \sum_{ijab} \int_{\text{BZ}} d\mathbf{k}_i \int_{\text{BZ}} d\mathbf{k}_a \int_{\text{BZ}} d\mathbf{k}_b \{ 2|Q(ijab\mathbf{k}_i\mathbf{k}_a\mathbf{k}_b)|^2 - \text{Re}[Q(ijab\mathbf{k}_i\mathbf{k}_a\mathbf{k}_b)Q^*(ijba\mathbf{k}_i\mathbf{k}_b\mathbf{k}_a)] \} / (\epsilon_{i\mathbf{k}_i}^{\text{HF}} + \epsilon_{jT(\mathbf{k}_a+\mathbf{k}_b-\mathbf{k}_i)}^{\text{HF}} - \epsilon_{a\mathbf{k}_a}^{\text{HF}} - \epsilon_{b\mathbf{k}_b}^{\text{HF}}), \quad (2)$$

where BZ denotes the first Brillouin zone in reciprocal space,  $W$  is the volume of the BZ,  $\epsilon_{p\mathbf{k}}^{\text{HF}}$  are HF orbital energies, and  $Q(ijab\mathbf{k}_i\mathbf{k}_a\mathbf{k}_b)$  are modified two-electron integrals over Bloch orbitals.

The optimized HF and MBPT(2) geometries with the basis set are the geometries at which  $E_{\text{uc}}^{\text{HF}}$  and  $E_{\text{uc}}^{\text{MBPT}(2)}$  have minimum values, respectively. There are many efficient algorithms developed to locate minima on potential energy surfaces.<sup>18,19</sup> Among them, the quadratic steepest descent line following algorithm<sup>20</sup> is more efficient and stable. The basic idea of this method is to construct a quadratic form using the energy and the gradient at the current point with an updated Hessian, then follow the steepest descent line of the quadratic form to the next point, and repeat this procedure until convergence is reached.

Optimized geometries or minima on potential energy surfaces correspond to molecular equilibrium structures. Besides their importance, they also provide the starting point for the determination of all other properties.

### B. Band gap

In an extended system, orbital energies  $\epsilon_{n\mathbf{k}}$  form the energy bands. According to Koopmans' theorem,<sup>21</sup> the HF band energies for occupied and unoccupied bands are equal to the corresponding HF ionization potentials and electron affinities, respectively. Beyond the HF approximation, one can still define the band energies as the ionization potentials for quasi-particle occupied orbitals and the electron affinities for unoccupied orbitals.<sup>22</sup>

The MBPT(2) orbital energies are defined as the MBPT(2) energy difference between the neutral and the ion systems and are given by

$$\epsilon_p^{\text{MBPT}(2)} = \epsilon_p^{\text{HF}} + \epsilon_p^{(2)}, \quad (3)$$

where  $\epsilon_p^{(2)}$  is the second-order MBPT correction to the band energy, which can be calculated by<sup>16</sup>

$$\epsilon_p^{(2)} = \left( \frac{1}{W} \right)^2 \sum_{iab} \int_{\text{BZ}} d\mathbf{k}_a \int_{\text{BZ}} d\mathbf{k}_b \{ 2|Q(piab\mathbf{k}_p\mathbf{k}_a\mathbf{k}_b)|^2 - \text{Re}[Q(piab\mathbf{k}_p\mathbf{k}_a\mathbf{k}_b)Q^*(piba\mathbf{k}_p\mathbf{k}_b\mathbf{k}_a)] \} / (\epsilon_{p\mathbf{k}_p}^{\text{HF}} + \epsilon_{jT(\mathbf{k}_a+\mathbf{k}_b-\mathbf{k}_i)}^{\text{HF}} - \epsilon_{a\mathbf{k}_a}^{\text{HF}} - \epsilon_{b\mathbf{k}_b}^{\text{HF}}) + \left( \frac{1}{W} \right)^2 \sum_{aij} \int_{\text{BZ}} d\mathbf{k}_i \int_{\text{BZ}} d\mathbf{k}_j \{ 2|Q(paij\mathbf{k}_p\mathbf{k}_i\mathbf{k}_j)|^2 - \text{Re}[Q(paij\mathbf{k}_p\mathbf{k}_i\mathbf{k}_j)Q^*(pajik_p\mathbf{k}_i\mathbf{k}_j)] \} / (\epsilon_{p\mathbf{k}_p}^{\text{HF}} + \epsilon_{aT(\mathbf{k}_i+\mathbf{k}_j-\mathbf{k}_p)}^{\text{HF}} - \epsilon_{i\mathbf{k}_i}^{\text{HF}} - \epsilon_{j\mathbf{k}_j}^{\text{HF}}). \quad (4)$$

The band gap in an extended system is defined as the difference between the lowest band energy in the conduction band and highest band energy for the valence band.<sup>22</sup> It determines whether the system is a conductor, a semiconductor or an insulator. The HF band gaps are much larger than the measured values due to the lack of electron correlation. Including electron correlation, MBPT(2) band gaps greatly improve the HF results although they are still larger than the experimental values, primarily because of the corresponding poor description of the conduction bands.

### C. Vibrational frequencies

Piseri and Zerbi<sup>23</sup> have developed the theory for vibrational motions of nuclei in an infinite periodic chain.<sup>23</sup> In the following, we will give the basic formulas to be used in our calculations.

Let  $\mathbf{r}_n$  and  $\mathbf{x}_n$  be the displacements of all internal and Cartesian coordinates, respectively, relative to the stable structure in the  $n$ th unit cell. Hence, we have the relationship

$$\mathbf{r}_n = \sum_l \mathbf{B}_l \mathbf{x}_{n+l}, \quad (5)$$

where  $\mathbf{B}_l$  are transformation matrices. Then the kinetic energy and potential energy for the system can be expressed as

$$T = \frac{1}{2} \sum_n \dot{\mathbf{x}}_n^\dagger \mathbf{M} \dot{\mathbf{x}}_n, \quad (6)$$

where  $M$  is the mass matrix which is diagonal, and

$$V = \frac{1}{2} \sum_{nn'} \mathbf{r}_n^\dagger \mathbf{F}_{nn'} \mathbf{r}_{n'}, \quad (7)$$

where  $\mathbf{F}_{nn'}$  are the force constants with respect to  $\mathbf{r}_n$  and  $\mathbf{r}_{n'}$ , respectively. The translational symmetry ensures that

$$\mathbf{F}_{nn'} = \mathbf{F}_{0n'-n}. \quad (8)$$

Using  $\mathbf{R}(k)$  and  $\mathbf{X}(k)$  to denote the symmetrized internal and Cartesian coordinates for translational symmetry. Then  $\mathbf{R}(k)$  and  $\mathbf{X}(k)$  can be calculated by

$$\mathbf{R}(k) = \frac{1}{\sqrt{2\pi/a}} \sum_n \mathbf{r}_n e^{-ikn/a} \quad (9)$$

and

$$\mathbf{X}(k) = \frac{1}{\sqrt{2\pi/a}} \sum_n \mathbf{x}_n e^{-ikn/a}, \quad (10)$$

respectively. The internal and Cartesian coordinates for the symmetrized coordinates  $\mathbf{R}(k)$  and  $\mathbf{X}(k)$  can also be calculated by

$$\mathbf{r}_n = \int_{-\pi/a}^{\pi/a} \frac{1}{\sqrt{2\pi/a}} e^{ikn/a} \mathbf{R}(k) dk, \quad (11)$$

$$\mathbf{x}_n = \int_{-\pi/a}^{\pi/a} \frac{1}{\sqrt{2\pi/a}} e^{ikn/a} \mathbf{X}(k) dk. \quad (12)$$

Substituting Eqs. (11) and (12) into Eqs. (6) and (7), one can get

$$T = \frac{1}{2} \int_{-\pi/a}^{\pi/a} \dot{\mathbf{X}}(k)^\dagger \mathbf{M} \dot{\mathbf{X}}(k) dk, \quad (13)$$

$$V = \frac{1}{2} \int_{-\pi/a}^{\pi/a} \mathbf{R}(k)^\dagger \mathbf{F}_R(k) \mathbf{R}(k) dk, \quad (14)$$

where

$$\mathbf{F}_R(k) = \sum_n \mathbf{F}_{0n} e^{ikn/a}, \quad (15)$$

and use has been made of Eq. (8) and

$$\frac{a}{2\pi} \sum_n e^{ikn/a} = \delta(k). \quad (16)$$

From Eqs. (5), (11), and (12), we can connect  $\mathbf{R}(k)$  and  $\mathbf{X}(k)$  by

$$\mathbf{R}(k) = \mathbf{B}(k) \mathbf{X}(k), \quad (17)$$

where

$$\mathbf{B}(k) = \sum_l e^{ikl/a} \mathbf{B}_l. \quad (18)$$

Substituting Eq. (17) into Eq. (14), we get

$$V = \frac{1}{2} \int_{-\pi/a}^{\pi/a} \mathbf{X}(k)^\dagger \mathbf{F}_X(k) \mathbf{X}(k) dk, \quad (19)$$

where

$$\mathbf{F}_X(k) = \mathbf{B}(k)^\dagger \mathbf{F}_R(k) \mathbf{B}(k). \quad (20)$$

Then the vibrational frequencies  $\omega(k)$  can be calculated by

$$\text{Det}[\mathbf{M}^{-1/2} \mathbf{F}_X(k) \mathbf{M}^{-1/2} - \omega(k)^2 \mathbf{I}] = 0, \quad (21)$$

where  $\mathbf{I}$  is an identity matrix. The rank of  $\mathbf{F}_X(k)$  is determined by the number of Cartesian coordinates in one unit cell, providing the same number of solutions for  $\omega(k)$  from Eq. (21). If there is an additional symmetry and only the vibrational modes for certain representations are of interest, the size of the matrix  $\mathbf{F}_X(k)$  becomes smaller. The solutions of Eq. (21) form the phonon dispersion curves which are analogous to energy bands. From the phonon dispersion curves, the density of the phonon states can be determined. From Eqs. (11) and (12), we can see that for a nucleus moving with a phase  $\phi$ , there is always a corresponding nucleus in another unit cell moving with a phase of  $-\phi$  in a vibrational mode with  $k \neq 0$  or  $\pi/a$ . Their contributions to the dipole moment always cancel each other. Then all vibrational motions for  $k \neq 0$  or  $\pi/a$  do not change the dipole moment. The corresponding vibrational modes are, therefore, not active and cannot be observed in infrared (IR) spectra.<sup>10</sup> For  $k=0$ , all the corresponding nuclei in different unit cells move in phase and their contributions to the dipole moment add. Since the value of the contribution from each unit cell is a function of the nuclei's coordinates, the dipole moment changes with the vibrational motion. Then the vibrational modes with  $k=0$  are observable in an IR spectra. The frequencies for these modes are called fundamental frequencies.

From Eq. (11), the translational symmetry is preserved when  $k=0$  and then

$$E_{\text{uc}} = E_{\text{uc}}^{\text{opt}} + \frac{1}{2} \sum_n \mathbf{r}_0^\dagger \mathbf{F}_{0n} \mathbf{r}_n = E_{\text{uc}}^{\text{opt}} + \frac{1}{2} \mathbf{r}^\dagger \mathbf{F}_R \mathbf{r}, \quad (22)$$

where  $E_{\text{uc}}$  can be either  $E_{\text{uc}}^{\text{HF}}$  or  $E_{\text{uc}}^{\text{MBPT}(2)}$ ,  $E_{\text{uc}}^{\text{opt}}$  is the total energy per unit cell at the optimized geometry  $\mathbf{r}_{\text{opt}}$ , and  $\mathbf{r}$  are the internal coordinates in any one unit cell. Taking the second derivatives on both sides of Eq. (22), we get

$$\{\mathbf{F}_R(0)\}_{ij} = \frac{\partial^2 E_{\text{uc}}}{\partial \gamma_i \partial \gamma_j}. \quad (23)$$

For a polymer with screw symmetry such as polyethylene, the vibrational modes for  $k = \pi/a$  may also be observed. Otherwise, the vibrational modes for  $k = \pi/a$  are not active in the IR spectra.

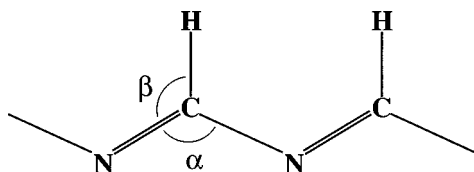


FIG. 1. The structure of polymethineimine and the five independent internal coordinates:  $r_{N=C}$ ,  $r_{C-N}$ ,  $r_{C-H}$ ,  $\alpha$ , and  $\beta$ .

### III. APPLICATION TO POLYMETHINEIMINE

PLH93 (Ref. 24) and PLMBPT (Ref. 16) programs are used for HF and MBPT(2) calculations, respectively. The number of unit cells for the lattice summations in both HF and MBPT(2) calculations is 21. Multipole expansions have been used in HF calculations for the lattice summations outside of the 21 unit cells to further enhance the convergence of the HF results.<sup>24</sup> The convergence of MBPT(2) for both the total energy per unit cell and for the quasi-particle band energies with the lattice summations have been studied in our previous report.<sup>16</sup> The total energy per unit cell converges much faster with the lattice sums than the quasi-particle band energies. For our current application, 21 unit cells in the lattice summations are sufficient to give reliable numerical results.

#### A. Stable structure

The structure of polymethineimine has not been determined by experiment yet. There are a few theoretical geometries for this polymer obtained by HF calculations with small and medium sized basis sets.<sup>5,6</sup> In the following, we will determine the geometry using both HF and MBPT(2) with different basis sets.

Figure 1 shows the structure of all-*trans* polymethineimine. It is in a plane and its unit cell is NCH. The five independent internal coordinates are  $r_{N=C}$ ,  $r_{C-N}$ ,  $r_{C-H}$ ,  $\alpha$ ,  $\beta$ . Among them,  $r_{N=C}$ ,  $r_{C-N}$ , and  $\alpha$  determine the unit cell length  $a$  by

$$a = \sqrt{r_{N=C}^2 + r_{C-N}^2 - 2r_{N=C}r_{C-N} \cos(\alpha)}. \quad (24)$$

Since analytical gradients are not yet available in PLH93 or other periodic HF packages, numerical gradients are used in our geometry optimizations. We take  $\Delta r_{N=C}$ ,  $\Delta r_{C-N}$ ,  $\Delta r_{C-H}$  to be 0.01 Å and  $\Delta\alpha$ ,  $\Delta\beta$  to be 0.4° in our calculations. To be sure that our optimized geometries are reliable, we have checked our results by doubling these step sizes and reducing them by half to assess the sensitivity of the numerical results, with no change in the accuracy of our reported data.

Table I compares our optimized HF geometries obtained with basis sets STO-3G and 6-31G for polymethineimine with those given by Teramae *et al.*<sup>6</sup> and Karpfen.<sup>5</sup> From the table, we can see that there is very good overall agreement between our results and theirs. But we also discern small differences. These differences may come from the different lattice summation cutoffs. As we mentioned above, we take 21 unit cells in our calculations plus a multipole expansion outside this region to enhance the convergence of the lattice

TABLE I. Comparison among optimized HF geometries with basis sets STO-3G and 6-31G for polymethineimine (Units: Å and deg).

	$r_{N=C}$	$r_{C-N}$	$r_{C-H}$	$\alpha$	$\beta$
STO-3G <sup>a</sup>	1.281	1.452	1.097	116.6	125.0
STO-3G <sup>b</sup>	1.280	1.465	1.107	116.9	125.3
6-31G <sup>a</sup>	1.266	1.384	1.088	120.3	121.8
6-31G <sup>c</sup>	1.259	1.388	1.095	121.0	...

<sup>a</sup>Calculated by using PLH93 with 21 unit cells.

<sup>b</sup>Reference 6.

<sup>c</sup>Reference 5.

summations. This should be contrasted with only 9 unit cells taken in Teramae *et al.*'s calculation and five in Karpfen's.

Table II lists the optimized geometries for both HF and MBPT(2) methods with three basis sets, STO-3G, 6-31G, and 6-31G\*\*\*. The bond length  $r_{C-H}$  does not change much with basis and method compared to the other internal coordinates. With increase of the basis set size, the two bond lengths  $r_{N=C}$  and  $r_{C-N}$  always decrease no matter whether HF or MBPT(2) is used in the calculation. The larger the basis the stronger the two bonds. The decrease of the two bond lengths also means an increase of the repulsion among the nitrogen nuclei, which causes an increase in  $\alpha$ . We can also see from Table II that the single bond between nitrogen and carbon atoms is more sensitive to the size of the basis than that of the double bond. The result is that the difference of the two bond lengths decreases with the increase in the basis set size. Since electron correlation typically diffuses the electron cloud, the correlated bond lengths tend to be larger than those obtained by HF with the same basis set. Because of the increase of the two bond lengths,  $r_{N=C}$  and  $r_{C-N}$ ,  $\alpha$  decreases and then  $\beta$  increases with inclusion of electron correlation. The double bond is more sensitive to electron correlation. This also results in a decrease in the difference between the two bond lengths,  $r_{N=C}$  and  $r_{C-N}$ .

#### B. Band gap

Polymethineimine was found to be a semiconductor in the early seventies, although its band gap was not accurately measured.<sup>1,2</sup> Since it has a conjugate structure similar to polyacetylene, polymethineimine became a candidate for a possible conducting material. Using the HF method with a small STO-3G basis, Teramae *et al.* predicted that polymethineimine had a very large band gap, suggesting that it

TABLE II. The optimized geometries for polymethineimine using both HF and MBPT(2) with three basis sets, STO-3G, 6-31G, and 6-31G\*\*\* (Units: Å and deg).

	$r_{N=C}$	$r_{C-N}$	$r_{C-H}$	$\alpha$	$\beta$
HF/STO-3G	1.2814	1.4515	1.0973	116.63	125.03
MBPT(2)/STO-3G	1.3367	1.4836	1.1190	113.76	126.33
HF/6-31G	1.2657	1.3839	1.0876	120.30	121.82
MBPT(2)/6-31G	1.3039	1.4098	1.1088	118.31	122.96
HF/6-31G***	1.2616	1.3617	1.0939	119.61	121.55
MBPT(2)/6-31G***	1.2859	1.3717	1.1023	118.19	122.16

TABLE III. Band gaps calculated using HF and MBPT(2) with three basis sets, STO-3G, 6-31G, and 6-31G\*\* (Unit: eV).

	$\epsilon_{v,\max}$	$\epsilon_{c,\min}$	$E_g$ (eV)
HF/STO-3G	-7.3126	2.7502	10.0628
MBPT(2)/STO-3G	-6.1099	2.1524	8.2623
HF/6-31G	-9.0705	-0.8250	8.2454
MBPT(2)/6-31G	-7.5709	-2.5668	5.0041
HF/6-31G**	-8.9331	-0.3900	8.5431
MBPT(2)/6-31G**	-7.6166	-2.8340	4.7826

would not be a good candidate system.<sup>6</sup> In the following, we will show that by augmenting the basis set and including electron correlation, the theoretical band gap will reduce dramatically.

The second column in Table III lists the HF and MBPT(2) quasi-particle orbital energies for the highest occupied orbital,  $\epsilon_{v,\max}$ , the absolute values of which are the first ionization potentials (IP) predicted by the corresponding combination of method and basis set. As expected,<sup>16</sup> electron correlation reduces the IP for all three basis sets. The IP does not change much when the basis set is enlarged from 6-31G to 6-31G\*\*. The third column gives the HF and MBPT(2) quasi-particle orbital energies for the lowest unoccupied orbital,  $\epsilon_{c,\min}$ , the negative values of which are theoretical electron affinities (EA). The larger the basis set, the stronger the electron attachment predicted by MBPT(2). However, the EA predicted by HF with 6-31G basis is larger than that obtained by HF with 6-31G\*\*. This shows that electron correlation is critical in the calculations of electron affinities. The IP and EA predicted by MBPT(2)/6-31G\*\* are 7.6166 and 2.8340 eV, respectively.

Table III lists the band gaps,  $E_g = \text{IP} - \text{EA}$ , obtained by using HF and MBPT(2) with the three different basis sets. The optimized geometry with the same method and basis is used in each calculation. The number of unit cells in the lattice summation is the same as that used in geometry optimization, namely 21. HF with a STO-3G basis predicts that the band gap is 10.0628 eV, which is much too large to match the obtained semiconducting property of polymethineimine. By increasing the size of the basis set, HF with 6-31G reduces the value by 1.8174 eV. But there is no further improvement when the larger basis set 6-31G\*\* is used. By including electron correlation through MBPT(2), the band gap is further reduced by 1.8005 eV for STO-3G, 3.2413 eV for 6-31G, and 3.7605 eV for 6-31G\*\*, respectively. The larger the basis set the larger the contribution of electron correlation to the band gap. The MBPT(2) band gap obtained with 6-31G\*\* is 4.7826 eV. Considering that the band gap of polyacetylene computed at the same level is 4.033 eV,<sup>16</sup> we can estimate that the real band gap of polymethineimine is about 0.75 eV larger than that of polyacetylene with the assumption of the same difference between MBPT(2)/6-31G\*\* calculation and experiment for the two systems. This provides an estimate of about 2.75  $\pm$  0.5 eV for the band gap. Analogously, if the gap is assumed to be associated with the first peak in the polymethine-

TABLE IV. Comparison between STO-3G HF vibrational frequencies (unit: 1/cm). Results are scaled by 0.89.

	C-N str.	C-H def.	C=N str.	C-H str.
Teramae <i>et al.</i> <sup>a</sup>	1152	1351	1669	3077
Ours <sup>b</sup>	1176	1334	1685	3109
Experiment <sup>c</sup>		1410	1620	3170

<sup>a</sup>Our calculation employs 21 unit cells plus multipole expansion outside the region compared to 9 in the Teramae *et al.* (Ref. 6).

<sup>b</sup>Reference 5.

<sup>c</sup>References 1 and 2.

neimine's absorption spectrum, it, too, would occur at about 2.75 eV, considering that the peak for polyacetylene appears at about 2 eV.<sup>25</sup>

### C. Vibrational frequencies

Three fundamental vibrational frequencies of polymethineimine were observed in the early seventies by Wöhrle.<sup>2</sup> Besides the semiconducting property, they are the only measured properties for polymethineimine. Using the HF method with basis set STO-3G, Teramae *et al.*<sup>6</sup> calculated the fundamental frequencies for polymethineimine. Teramae *et al.*'s numerical and Wöhrle's measured vibrational frequencies are listed in the first and third rows in Table IV. The theoretical results were scaled by a factor of 0.89. With the scaling, Teramae *et al.*'s numerical results match the observed values reasonably well. However, reliable theoretical results can only be obtained with a basis set that is large enough to get the results sufficiently converged, and with the inclusion of electron correlation. In the following, we will calculate the fundamental vibrational frequencies using both HF and MBPT(2) with three basis sets, STO-3G, 6-31G, and 6-31G\*\*.

The structure of all-*trans* polymethineimine is described in Fig. 1 and the internal coordinates optimized with the combinations of two methods and three basis sets are listed in Table II. Since the stable structure is a plane, all-*trans* polymethineimine has  $C_s$  symmetry besides its translational invariance.  $C_s$  symmetry has two irreducible representations,  $A'$  and  $A''$ , which categorize the normal modes.

The unit cell for all-*trans* polymethineimine is NCH. Then there are nine Cartesian coordinates in each cell. We denote them as  $x_N, y_N, z_N, x_C, y_C, z_C, x_H, y_H, z_H$ , taking the  $z$  axis to be perpendicular to the plane of polymethineimine. Then  $x_N, y_N, x_C, y_C, x_H, y_H$  are  $A'$  representations of  $C_s$  symmetry while  $z_N, z_C, z_H$  are  $A''$  representations. For fundamental vibrational modes, translational invariance is always kept. Then only one among  $r_{C-N}$  and  $\alpha$  is independent since the unit cell length is known and fixed. Therefore, there are only four internal coordinates,  $r_{N=C}, r_{C-N}, r_{C-H}$ , and  $\beta$ , belonging to  $A'$  and there are four  $A'$  normal modes which have non-zero frequencies. It is easy to see that for the  $A''$  representation there is only one internal coordinate  $\gamma$ , the angle between the carbon-hydrogen bond and the plane of the polymer. Then there is one normal mode with non-zero

TABLE V. Fundamental vibrational frequencies with symmetry  $A'$  calculated with different methods and basis sets (unit:1/cm). Unscaled.

	C-N str.	C-H def.	C=N str. <sup>a</sup>	C-H str.
HF/STO-3G	1305.94	1517.19	1866.66	3576.59
MBPT(2)/STO-3G	1014.92	1352.07	1505.99	3340.30
HF/6-31G	1257.19	1527.82	1696.89	3176.84
MBPT(2)/6-31G	1173.12	1396.08	1596.59	2957.92
HF/6-31G**	1140.57	1379.49	1607.04	3135.55
MBPT(2)/6-31G**	1009.77	1265.55	1582.76	2996.73
Experiment <sup>b</sup>		1410	1620	3170

<sup>a</sup>C-H def. (in plane) is mainly described by coordinate  $\beta$ .

<sup>b</sup>References 1 and 2.

frequency for  $A''$ . In the following, we only consider the normal modes for  $A'$  representations since their frequencies have been measured.

Our HF/STO-3G vibrational frequencies calculated with the geometry given by Teramae *et al.* are given in the second row of Table IV. To compare with Teramae *et al.*'s results, the frequencies listed in the row have been scaled by a factor 0.89 as they did for their data. The two calculations agree well. In fact, since the numbers of unit cells used in the lattice summations of the two calculations were not the same, this causes some differences. Considering this, we can see that the error induced by the numerical gradient and Hessian are sufficiently small for our current application.

Table V provides our calculated fundamental vibrational frequencies for all-*trans* polymethineimine. The vibrational frequencies listed in each row are calculated by the combination of method and basis given in the first column at the corresponding optimized structure listed in Table I. The numerical vibrational frequencies given in Table V have not been scaled by any factor. From the table, we can see that both basis set and electron correlation have a large influence on numerical vibrational frequencies. We have carefully checked the influence of the step size used for numerical gradient and hessian calculations on our vibrational frequencies. The error induced by numerical derivatives should be around  $10 \text{ cm}^{-1}$ .

For STO-3G, the HF vibrational frequencies are larger than the experimental values. MBPT(2) improves the numerical results by a few hundred wave numbers. When the 6-31G basis is used, both HF and MBPT(2) provide good agreement with experiment. In fact, the agreement is better than would be expected or that the methods can achieve in finite systems. If we look further at the data, we find that the HF results are larger while MBPT(2) values are smaller than the observed frequencies. When the larger basis set 6-31G\*\* is used, MBPT(2) frequencies are even smaller than those obtained with 6-31G, although MBPT(2)/6-31G\*\* frequencies still match the measured values reasonably well. If one just looks at the differences between them, their agreement is at the level that MBPT(2) can obtain in finite systems. The difference is that in finite systems, the vibrational frequencies calculated with MBPT(2)/6-31G\*\* are almost invariably larger than those

observed<sup>11</sup> while here the situation is the opposite. However, it is not clear that the experimental results are for pure all-*trans* polymethineimine, as other *cis-transoid* and *trans-cisoid* structures are possible. To clarify this issue, theoretical study about other isomers of polymethineimine besides all-*trans* and further experiments are needed.

## IV. CONCLUSIONS

Using both HF and MBPT(2) with basis sets STO-3G, 6-31G, and 6-31G\*\*, we have optimized the geometries for polymethineimine. Both basis set and electron correlation have a strong effect on the equilibrium structure of the system. Either basis set improvements or including electron correlation reduces the difference between the single and double carbon-nitrogen bond lengths.

For the band gap, the larger the basis set, the smaller the band gap in both methods. However, the band gap obtained by HF with 6-31G\*\* is still 8.54 eV. Electron correlation has a dramatic effect on the band gap, with MBPT(2) giving 4.78 eV for the band gap.

We have also calculated the fundamental vibrational frequencies for polymethineimine using HF and MBPT(2) with three basis sets. The theoretical results match the measured values very well when a large basis is used. The comparison among theoretical and experimental vibrational frequencies also indicates that the interaction among different chains may be non-negligible.

## ACKNOWLEDGMENTS

We would like to thank Dr. M. Nooijen for valuable comments. This work is supported by the U.S. Office of Naval Research under Grant No. N00014-92-J-1100.

<sup>1</sup>D. Wöhrle, *Tetrahedron Lett.* **1969** (1971).

<sup>2</sup>D. Wöhrle, *Makromol. Chem.* **175**, 1751 (1974).

<sup>3</sup>C. K. Chiang *et al.*, *Phys. Rev. Lett.* **39**, 1098 (1977).

<sup>4</sup>D. Jacquemin, B. Champagne, J.-M. André, and B. Kirtman, *Chem. Phys.* **213**, 217 (1996).

<sup>5</sup>A. Karpfen, *Chem. Phys. Lett.* **64**, 299 (1979).

<sup>6</sup>H. Teramae, T. Yamabe, and A. Imamura, *J. Chem. Phys.* **81**, 3564 (1984).

<sup>7</sup>I. D. L. Albert, S. Ramasesha, and P. K. Das, *Phys. Rev. B* **43**, 7013 (1991).

<sup>8</sup>J. L. Brédas, B. Thémans, and J. M. André, *J. Chem. Phys.* **78**, 6137 (1983).

<sup>9</sup>G. Herzberg, *Infrared and Raman Spectra of Polyatomic Molecules* (Van Nostrand, New York, 1945); L. M. Sverdlov, M. A. Kovner, and E. P. Krainov, *Vibrational Spectra of Polyatomic Molecules* (Wiley, New York, 1974).

<sup>10</sup>J. L. Koenig, *Spectroscopy of Polymers* (American Chemical Society, Washington, D.C., 1992).

<sup>11</sup>R. J. Bartlett and J. F. Stanton, *Applications of Post-Hartree-Fock Methods: A Tutorial*, Vol. 5 in *Reviews in Computational Chemistry*, edited by K. B. Lipkowitz and D. B. Boyd (VCH, New York, 1994), pp. 65–169.

<sup>12</sup>J. J. Ladik, *Quantum Theory of Polymers as Solids* (Plenum, New York, 1988).

<sup>13</sup>H. P. Kelly, *Adv. Chem. Phys.* **14**, 129 (1969); R. J. Bartlett, *Annu. Rev. Phys. Chem.* **32**, 359 (1981), and references therein.

<sup>14</sup>J. Cizek, *Adv. Chem. Phys.* **14**, 35 (1969); R. J. Bartlett, *J. Phys. Chem.* **93**, 1697 (1989); *Coupled-Cluster Theory: An Overview of Recent Devel-*

- opments in *Modern Electronic Structure Theory*, edited by D. R. Yarkony (World Scientific, New Jersey, 1995), pp. 1047–1131, and references therein.
- <sup>15</sup> Suhai, *Phys. Rev. B* **27**, 3506 (1983); *Int. J. Quantum Chem.* **42**, 193 (1992).
- <sup>16</sup> J. Q. Sun and R. J. Bartlett, *J. Chem. Phys.* **104**, 8553 (1996).
- <sup>17</sup> J. Q. Sun and R. J. Bartlett, *Phys. Rev. Lett.* **77**, 3669 (1996).
- <sup>18</sup> H. B. Schlegel, *Adv. Chem. Phys.* **67**, 249 (1987).
- <sup>19</sup> J. D. Head and M. C. Zerner, *Adv. Quantum Chem.* **20**, 239 (1989).
- <sup>20</sup> J. Q. Sun, K. Ruedenberg, and G. J. Atchity, *J. Chem. Phys.* **99**, 5276 (1993).
- <sup>21</sup> T. A. Koopmans, *Physica* **1**, 104 (1933).
- <sup>22</sup> S. T. Pantelides, A. J. Mickish, and A. B. Kunz, *Phys. Rev. B* **10**, 2602 (1974).
- <sup>23</sup> L. Piseri and G. Zerbi, *J. Mol. Spectrosc.* **26**, 254 (1961).
- <sup>24</sup> J. M. Andre *et al.*, in METEXX-94, *Methods and Techniques in Computational Chemistry*, edited by E. Clementi (Stef, Cagliari, 1993), Vol. B, Chap. 10, pp. 423–480; J. M. André, D. H. Mosley, B. Champagne, J. Delhalle, J. G. Fripiat, and J. L. Brédas, *LCAO AB Initio Band Structure Calculations for Polymers (PLH93)*.
- <sup>25</sup> S. Etemad, A. J. Heeger, L. Lauchlan, T. C. Chung, and A. G. MacDiarmid, *Mol. Cryst. Liq. Cryst.* **77**, 43 (1981).